CHANDRA
X-ray Center 60 Garden St., Cambridge Massachusetts 02138 USA

MEMORANDUM

Date: January 22, 2002

From: Beth Biller, Paul Plucinsky, Richard Edgar

To:
Subject: Using Chandra Level 0 Event Histogram Files to Characterize the High-Energy Particle Background
Re:
Cc:
File: `hist_writeup.tex`
Version: `3.3`

Abstract

We have analyzed ∼30 ACIS data sets collected in "Event Histogram" mode in order to characterize the background of the S3 and I3 CCDs produced by high-energy charged particles. We have computed count rates in four energy bands (0.5-2.0 keV, 0.5-7.0 keV, 5.0-10.0 keV, and 0.3-10.0 keV) at the bottom and top of the CCDs. We have determined that the S3 background is flatter, albeit higher, than the I3 background which exhibits a 20% increase from bottom to top. We have created composite background spectra for both CCDs. These spectra have dramatically different shapes and features for the BI and FI CCDs. We have also investigated the time variability of this background and have found that this component varied by ∼20% over the $1\,\frac{1}{4}$ year interval considered. We have also compared the composite background spectra to the background data from sky observations and from the Dark Moon pointings. We find an excellent agreement between Event Histogram spectra and the Dark Moon spectra.

1 Event Histogram Mode Data

For exposure times longer than 5 ks where HRC is in the focal plane, ACIS collects data in "Event Histogram" mode. In this mode, ACIS identifies events in exactly the same manner as "Timed Exposure" mode, but instead of reporting individual events, ACIS accumulates pulse-height distributions (spectra) of the *summed* pulse height of the accepted events. Using the current parameter blocks (PB), only events with ASCA grades 0, 2, 3, 4, and 6 are accepted and data are acquired in 1650 frame (5,348s) intervals. Two such parameter blocks have been used through June 2001, one (WT0023C014, PB ID #=2342932) accepts events from the top 201 rows (rows 801-1001) and the other (WT0023A014, PB ID #=2334740) accepts events from the bottom 201 rows (21-221) of the CCD. Only five CCDs are used during these runs: I1-I3, S2 and S3. Separate event histogram files are produced for each node of the active CCDs. After June 2001, the Event Histograms will be acquired from the entire quadrant if the SIM is at the HRC-I position. Since the flux from cosmic X-rays focussed by the HRMA is zero and the flux from the external calibration source is negligible while the SIM is at the position which puts the HRC-I into the focus of the HRMA, these data can be used to characterize the background produced by high-energy particles.

We analyzed composite front-side (I3) and back-side (S3) spectra derived from these histogram files. We selected the longest exposures available, especially focusing on observations longer than 60 ks. Only observations done with ACIS at -120 C were considered. Table 1 contains a summary of the OBSIDS we selected.

Table 1: Summary of OBSIDS

Obsid	Observation Date (yy/mm/dd)	Exposure Time ksec	Part of Chip
26	00-02-04	62.8	bottom
27	00-02-15	48.6	top
87	00-04-24	29.8	top
142	00-02-16	24.5	bottom
328	00-02-12	9.8	bottom
364	00-02-21	44.7	bottom
437	00-02-13	24.1	top
438	00-02-16	9.8	bottom
557	00-02-14	8.4	top
562	00-02-14	7.5	bottom
607	00-07-10	5.6	top
612	00-09-11	5.2	bottom
738	00-02-12	27.0	bottom
742	00-02-13	19.8	bottom
756	00-02-11	45.8	bottom
848	00-03-11	4.8	bottom
849	00-05-26	10.4	top
964	00-03-02	124.8	bottom
999	01-03-05	17.8	top
1004	01-01-12	11.8	bottom
1515	00-02-03	4.8	top
1549	01-01-15	5.6	top
1555	01-03-09	7.6	top
1670	01-03-05	18.3	bottom
1735	00-06-21	9.5	top
1736	00-06-21	8.5	bottom
1741	00-06-22	7.2	top
1862	00-12-18	35.7	bottom
1918	00-10-27	10.0	bottom
2430	01-03-24	10.5	bottom

Table 2: Total Event Histogram Countrates (countrates in rows 21-221 plus countrates in rows 801-1001) in Various Energy Bands on S3 and I3

chip	0.5-2 keV	0.5-7 keV	5-10 keV	0.3-10 keV
S3	0.042	0.120	0.185	0.298
I3	0.022	0.066	0.042	0.111

2 Data

2.1 Energy Band Sums

To determine the intensity of the particle background across the bandpasses typically used for analysis of Chandra data, we calculated total count rates for a number of broad spectral bands. The bands considered were 0.3-10 keV, 0.5-2 keV, 0.5-7 keV, and 5-10 keV. These bands allow a direct comparison to background rates from ACIS sky background spectra (Markevitch, 1999). Rates were determined for all 402 rows considered (rate in rows 21-221 plus rate in rows 801-1001, Table 2) and each node and section (either rows 21-221 or 801-1001) of the S3 and I3 chips (Table 3 to Table 6). Rates were calculated by summing together all appropriate event histograms across multiple obsids. PHA bins were converted into keV using the acisD2000-01-29gainN003.fits gain file from the CALDB. Since the detector in histogram mode does not record the location of each event on the chip, we created average gain correction tables for the top (rows 21-221) and bottom (rows 801-1001) of each chip. We performed two additional corrections on the event histogram data in order to mimic the grade selection and gain correction used with event mode data. Specifically we: 1) subtracted bad columns from the relevant ACIS background event files (Markevitch, 1999) and 2) fitted lines in the event histogram data taken when HRC-S was in the focal plane, using these fits to tweak the released gain table. (When HRC-S is in the focal plane, ACIS sits directly below the external calibration source, providing excellent emission lines for energy calibration.) The released gain table was adjusted by less than 1%. We are currently investigating the cause of this slight gain difference between the Event Histogram mode data and the Timed Event mode data.

We find significant node to node variation on both S3 and I3. This variation stems from the difference in grade selection between event histogram data and event file data. Various bad columns and pixels are removed during standard data processing from event file data. The lack of spatial data for each event precludes a similar removal for event histogram data. We have attempted to mimic bad column removal by subtracting out the rates extracted from the node boundary columns of ACIS sky backgrounds from the event histogram data. However, other bad columns and pixels remain in the data. This causes separate nodes on each chip to vary significantly in background with respect to each other.

The count rates in the standard energy bands reflect significance divergence in behavior between different chips. The background on S3 is twice that on I3 across all four energy bands. We observe energy dependent differences as well. On S3, the largest share of total counts within the 0.3-10 keV energy band falls into the 5-10 keV energy band. I3 receives higher countrates at moderate energies, with countrates in the 0.5-7 keV band comprising the majority of the total countrate from 0.3-10 keV. We consider the ratio of the 5-10 keV band to the 0.5-7 keV band (the two bands closest in width in energy space) in order to more quantitatively determine the high vs. low energy response of various sections of the I3 and S3 chips. These ratios are listed in Table 7. The high-energy component clearly dominates on S3.

To determine the intensity difference in the observed particle background between the top and the

Table 3: Countrates in Various Energy Bands for Rows 21-221 on S3

node	0.5-2 keV	0.5-7 keV	5-10 keV	0.3-10 keV
0	5.351e-03 ± 1.195e-04	1.568e-02 ± 1.941e-04	2.189e-02 ± 2.189e-04	3.555e-02 ± 2.887e-04
1	5.299e-03 ± 1.313e-04	1.568e-02 ± 2.031e-04	2.418e-02 ± 2.299e-04	3.882e-02 ± 3.129e-04
2	5.184e-03 ± 1.308e-04	1.580e-02 ± 2.041e-04	2.531e-02 ± 2.397e-04	3.974e-02 ± 3.150e-04
3	5.059e-03 ± 1.141e-04	1.577e-02 ± 1.940e-04	2.621e-02 ± 2.397e-04	4.003e-02 ± 3.030e-04
sum	2.089e-02 ± 2.483e-04	6.293e-02 ± 3.978e-04	9.760e-02 ± 4.644e-04	1.541e-01 ± 6.101e-04

Table 4: Countrates in Various Energy Bands for Rows 801-1001 on S3

node	0.5-2 keV	0.5-7 keV	5-10 keV	0.3-10 keV
0	5.138e-03 ± 1.814e-04	1.435e-02 ± 2.929e-04	2.238e-02 ± 3.554e-04	3.631e-02 ± 4.606e-04
1	6.361e-03 ± 2.050e-04	1.714e-02 ± 3.244e-04	2.342e-02 ± 3.650e-04	4.037e-02 ± 5.293e-04
2	5.278e-03 ± 1.943e-04	1.452e-02 ± 3.0373e-04	2.240e-02 ± 3.600e-04	3.757e-02 ± 5.084e-04
3	5.319e-03 ± 1.797e-04	1.444e-02 ± 2.912e-04	2.492e-02 ± 3.742e-04	3.853e-02 ± 4.715e-04
sum	2.210e-02 ± 3.807e-04	6.0454e-02 ± 6.066e-04	9.311e-02 ± 7.275e-04	1.528e-01 ± 9.864e-04

Table 5: Countrates in Various Energy Bands for Rows 21-221 on I3

node	0.5-2 keV	0.5-7 keV	5-10 keV	0.3-10 keV
0	2.340e-03 ± 9.726e-05	7.291e-03 ± 1.478e-04	7.048e-03 ± 1.253e-04	1.296e-02 ± 1.925e-04
1	2.787e-03 ± 1.306e-04	8.034e-03 ± 1.799e-04	7.185e-03 ± 1.294e-04	1.378e-02 ± 2.252e-04
2	2.431e-03 ± 1.268e-04	7.738e-03 ± 1.766e-04	7.176e-03 ± 1.288e-04	1.350e-02 ± 2.212e-04
3	2.406e-03 ± 9.755e-05	7.499e-03 ± 1.467e-04	7.038e-03 ± 1.249e-04	1.303e-02 ± 1.895e-04
sum	9.964e-03 ± 2.283e-04	3.056e-02 ± 3.269e-04	2.845e-02 ± 2.542e-04	5.327e-02 ± 4.154e-04

Table 6: Countrates in Various Energy Bands for Rows 801-1001 on I3

node	0.5-2 keV	0.5-7 keV	5-10 keV	0.3-10 keV
0	3.140e-03 ± 1.633e-04	9.310e-03 ± 2.525e-04	8.362e-03 ± 2.179e-04	1.522e-02 ± 3.120e-04
1	3.384e-03 ± 2.027e-04	9.464e-03 ± 2.8477e-04	8.663e-03 ± 2.2437e-04	1.553e-02 ± 3.414e-04
2	3.223e-03 ± 1.931e-04	9.3472e-03 ± 2.791e-04	8.401e-03 ± 2.222e-04	1.505e-02 ± 3.334e-04
3	3.028e-03 ± 1.618e-04	9.377e-03 ± 2.522e-04	8.502e-03 ± 2.201e-04	1.530e-02 ± 3.119e-04
sum	1.277e-02 ± 3.623e-04	3.750e-02 ± 5.351e-04	3.393e-02 ± 4.422e-04	6.110e-02 ± 6.499e-04

Table 7: Ratio of 5-10 keV/0.5-7 keV band

node	S3 bottom	S3 top	I3 bottom	I3 top
0	1.396	1.560	0.967	0.898
1	1.542	1.366	0.894	0.915
2	1.602	1.542	0.927	0.899
3	1.663	1.726	0.938	0.907

bottom of each chip we consider the ratio of the count rate at the top of each chip to the count rate at the bottom of the corresponding chip. Node to node variations have been averaged out. Table 8 contains the relevant ratios. While countrates between the top and the bottom of the chip are nearly identical on S3 ($\leq$ 5% variation), I3 displays more dramatic variation ($\leq$ 25% variation). These clear differences across the chips are reflected in the structure of spectra derived from the level 0 histogram files.

2.2 Composite FI(I3) and BI(S3) Spectra

We derived composite spectra by summing together all of the event histograms for rows 21-221 and rows 801-1001 on the S3 and I3 chips. (The high-energy particle background varies by $\sim$20% or less in the 0.3-10 keV band between observations. Thus, spectra can be reliably co-added. For more detail, see section III.) Composite spectra for the top and bottom sections of S3 and I3 are available in Figures 1 through 4 respectively. For the S3 chip, differences in count rate are negligible between the top and bottom of the chip. In contrast, the top of the I3 chip receives considerably higher count rates than the bottom.

The background spectra for S3 (figures 1 and 2) are primarily flat from 2-7 keV. The spectra rise by a factor of 8 between 7-10 keV. At low energies ($\leq$ 0.5 keV), the background rises steeply to 0.3 keV and then turns over. Spectra from the top and bottom of the chip agree to within 5%, except at energies greater than 10 keV, where the background is higher at the bottom of the chip. Line structure is apparent at $\sim$2 keV (Al Kα, Si Kα fluorescence, and Au M complex) and from 9.7 keV to 11.6 keV (Au Lα,β). A nickel feature is apparent at 8 keV. Ti Kα and Mn Kα appear at around 4.5 and 5.9 keV

Table 8: Top/Bottom countrate for the S3 and I3 chips

chip	0.5-2 keV	0.5-7 keV	5-10 keV	0.3-10 keV
S3	1.058	0.961	0.954	0.991
I3	1.282	1.227	1.193	1.147

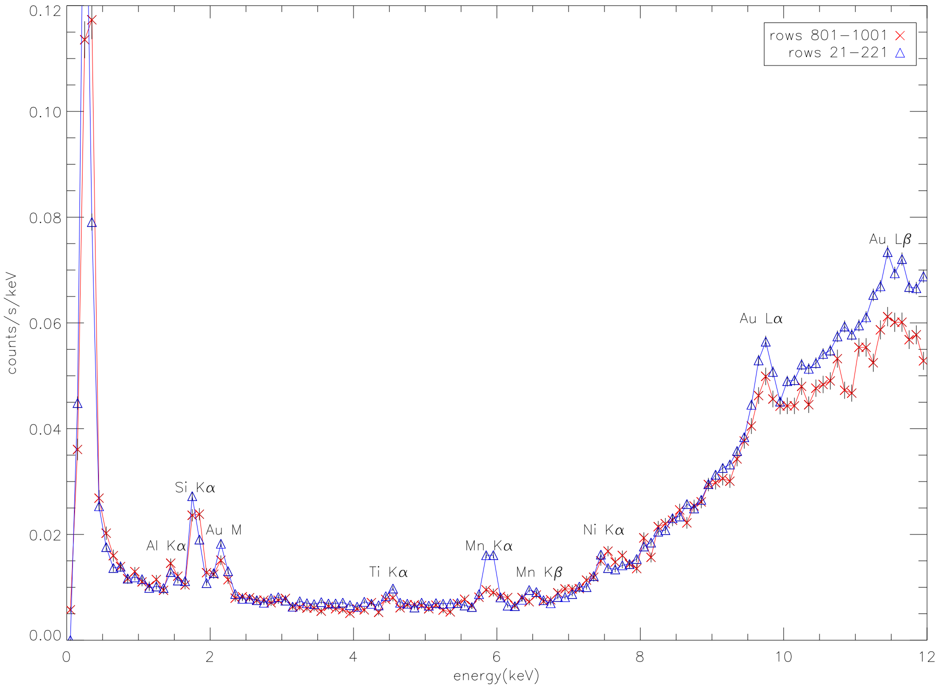

Figure 1: Composite Histogram Mode Background Spectra for the S3 chip. Energy is binned in units of 0.1 keV. Notable spectral features are labeled.

respectively. The Al Kα, Ti Kα, and Mn Kα lines stem from contamination by the external calibration source.

The event histogram background on I3 is dramatically smaller than that on S3, by nearly a factor of 2. (Spectra are in figures 3 and 4.) We observe a flatter spectrum overall from I3, with more striking line features. The background is somewhat higher at the top of the chip than at the bottom (on the order of 20%). We observe Al Kα, Si Kα fluorescence, and Au M complex lines at energies from 1.5 keV to 2.5 keV. A clear Ni Kα line is apparent at 7.5 keV and Au Lα,β appear at 9.7 keV and 11.5 keV respectively. Ti Kα and Mn Kα are also apparent at around 4.5 and 5.9 keV respectively. Again, Al Kα, Ti Kα, and Mn Kα lines are most likely due to contamination from the external calibration source.

Considerable differences exist in the shape of spectra from the top and bottom of the I3 chip. Three interesting features at 2.5 keV, 8.5 keV, and 10.8 keV appear in the spectrum from the top of the CCD but not from the bottom. We attribute these lines to Au M, Ni Kα, and Au Lα X-rays which have converted in the framestore region. The framestore shield has a Au coating with a Ni undercoating. Since the CTI is essentially zero in the framestore, the charge packets from these X-ray events do not suffer any losses in the transfer process. The observed energy of these lines is higher than the true value

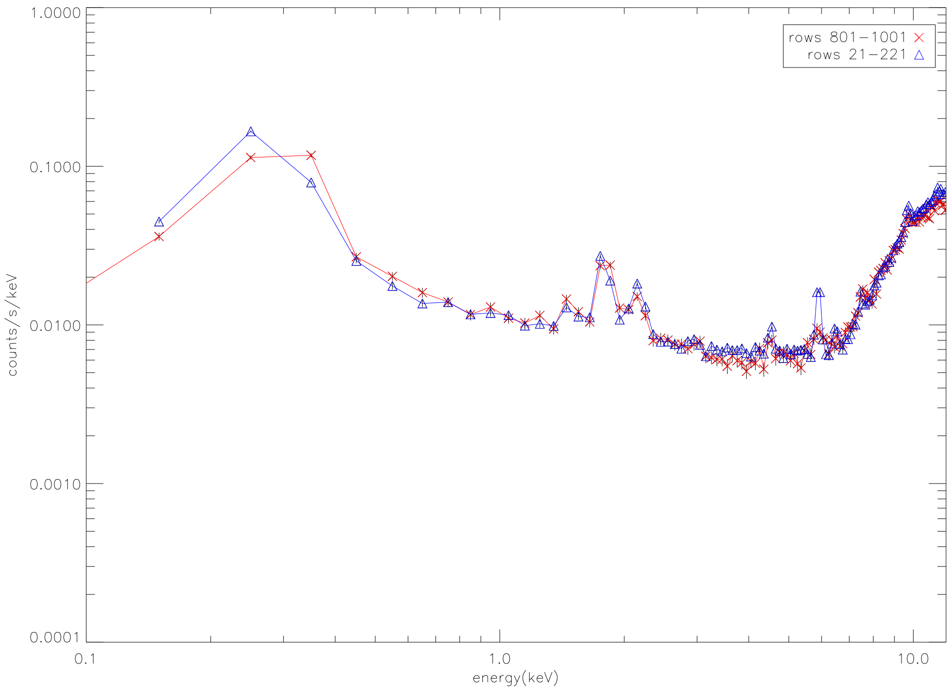

Figure 2: Composite Histogram Mode Background Spectra for the S3 chip. Energy is binned in units of 0.1 keV. X and Y axes are plotted logarithmically.

because the gain correction we have applied assumes these events converted in the imaging region where the charge packets are subject to CTI losses. At energies less than 1 keV, the spectra for the top and bottom diverge sharply, with the background at the bottom of the chip rising gently at lower energies while the background at the top plummets. This is due to very real charge transfer differences between the top and the bottom of the chip. At the top of the chip, the effects of CTI are much larger. The turnover seen at the lowest energies is caused by the lowest energy events losing enough charge that they fall below the event detection threshold.

3 Time Variability of the High Energy Particle Background

In this study, we consider both short-term and long-term time variability of the high-energy particle background. We define short-term variability to be that which occurs on timescales of thousands of seconds - in other words, time variability as observed within one observation. Long-term variability refers to variability over timescales of weeks or months – i.e., variability of the background from observation to observation.

It is important to note that for the study of time variability, only a basic gain correction (as described in Section II) was performed on the event histogram data. We did not subtract out hot columns from the ACIS sky backgrounds and used the released gain curve without any additional corrections.

We consider the short-term variability for the energy ranges considered in section II. Figures 5 and 6 contain counts per histogram file as a function of time for the S3 and I3 chips respectively during obsid 964, the longest bottom (rows 21-221) observation. Figures 7 and 8 contain counts per histogram file as a function of time for the S3 and I3 chips respectively during obsid 27, the longest top (rows

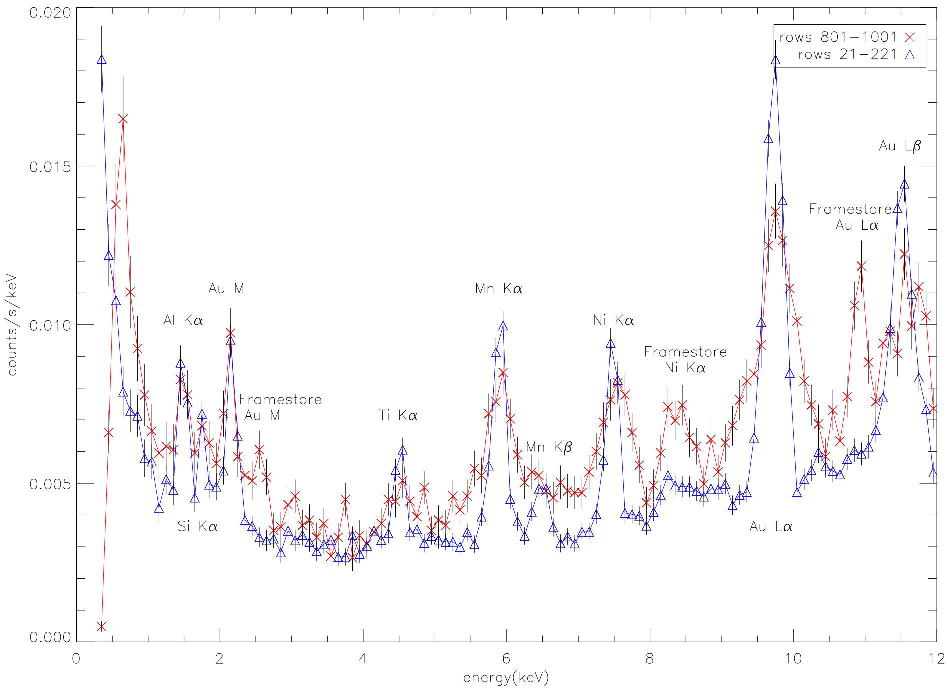

Figure 3: Composite Histogram Mode Background Spectra for the I3 chip. Energy is binned in units of 0.2 keV. Notable spectral features are labeled.

801-1001) observation. Each individual histogram file has an exposure time of about 5 ksec. Significant variation occurs within the high-energy particle background over the course of each observation. The high-energy particle background varies considerably more during obsid 964 than obsid 27. The counts received in the 0.3-10 keV band on the S3 chip displays variations of $\leq$ 14% ($\sim$100 counts) during obsid 964, but only $\leq$ 6% ($\sim$50 counts) during obsid 27.

For obsid 964, background variability is concentrated in intermediate energies (0.5-7 keV). (In other words, the general trend in counts in the 0.5-7 keV band clearly correllates to that in the full 0.3-10 keV band.) We find less variability at high (5-10 keV) and low (0.5-2 keV) energies. Comparing these 4 bands, we conclude that the observed short term variability occurs in the 2-5 keV range.

Similar correllated variability appears on the S3 chip during obsid 27 (Fig. 7). Background variability appears to be concentrated at lower energies, in the 0.5-2 and 0.5-7 keV bands. We observe no appreciable correllation in variability on I3 during obsid 27 (Fig. 8).

To test for long-term variability in the high-energy particle background, we consider the total count rate in a number of energy bands (0.3-10 keV, 5-10 keV, 0.5-2 keV, and 0.5-7 keV) across multiple observations. Figures 9 and 10 display counts/s in a number of bands on the S3 and I3 chip as a function of days since 1999-01-01. These plots possess two noteworthy features: 1) count rate in a number of bands decreases slightly with time and 2) the top of each chip uniformly receives somewhat higher countrates than the bottom of the chip. A couple of obsids (557 and 1515) produce anomalous high and low points. We will be investigating both these obsids separately; in this memo, we discard them for the purpose of constraining long-term variability. In the 0.3-10 keV band, we find count rate variations of up to 16% for rows 801-1001 on S3 and variations of up to 19% for rows 21-221. In the same band on I3, we find variations of up to 20% for rows 801-1001 and up to 35% for rows 21-221.

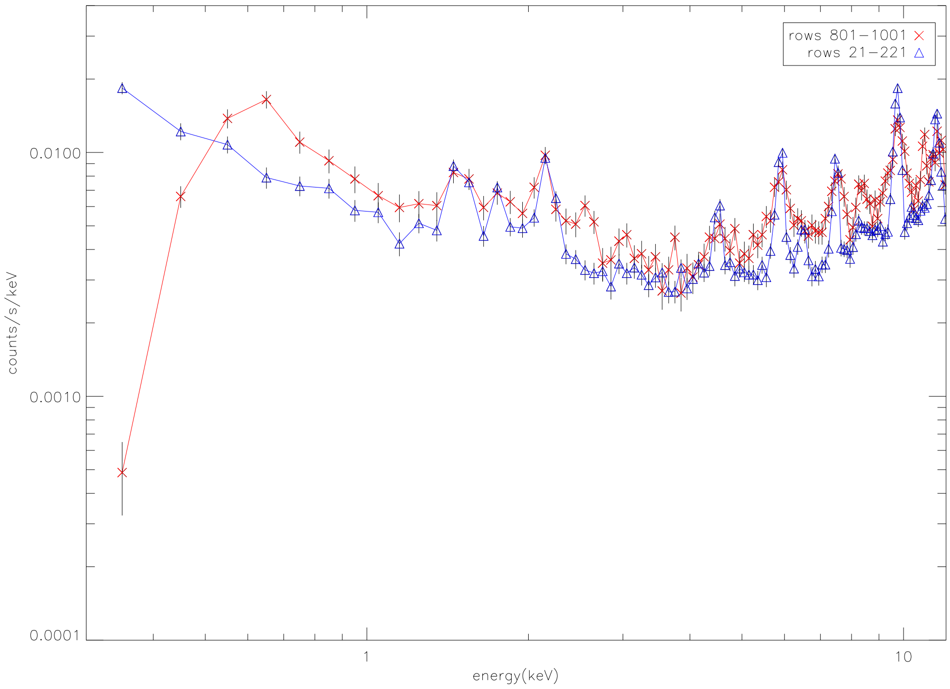

Figure 4: Composite Histogram Mode Background Spectra for the I3 chip. Energy is binned in units of 0.2 keV. X and Y axes are plotted logarithmically.

4 Comparison with Other Background Studies

We compare our results with the ACIS sky backgrounds derived by Markevitch (1999) and backgrounds generated from dark moon observations. In general, all three spectra look identical at energies greater than 2 keV. In Figures 11 to 14 background spectra derived from the level 0 event histogram files and corrected to represent the entire chip are overplotted with ACIS sky background spectra as well as spectra from dark moon observations (Markevitch, 2001) for S3. Difference in gain across the chip leads to some difficulty comparing the energy scales of different spectra. Gain corrections for the event histogram background spectra utilized gain tables averaged over the appropriate 201 rows on the chip and further corrected using line fits to event histogram data taken with HRC-S in the focal plane, whereas full gain tables, arfs, and rmfs were used to make gain corrections for the ACIS sky background spectra and moon spectra. Bad columns from the ACIS sky background spectra were subtracted from the event histogram data in order to better mimic level 2 event file event filtering.

On S3 (Figures 11 and 12), the ACIS sky background, moon observation background and event histogram background are statistically identical at energies greater than 2 keV. At energies less than 2 keV, we observe an excess of emission in the sky background relative to moon and event histogram backgrounds; this is presumably the Galactic X-ray background or unresolved point sources. A number of spectral features appear in all three spectra: 1) a feature at about 2 keV from the combined Al Kα, Si Kα, and Au Mα, β lines and 2) features at 9.7 keV to 11.6 apparent in all spectra from the Au Lα,β lines. Some notable differences exist between the spectra. The event histogram spectra display Mn K features between 5-7 keV. These features are due to residual calibration source flux and are not observed in the ACIS sky background.

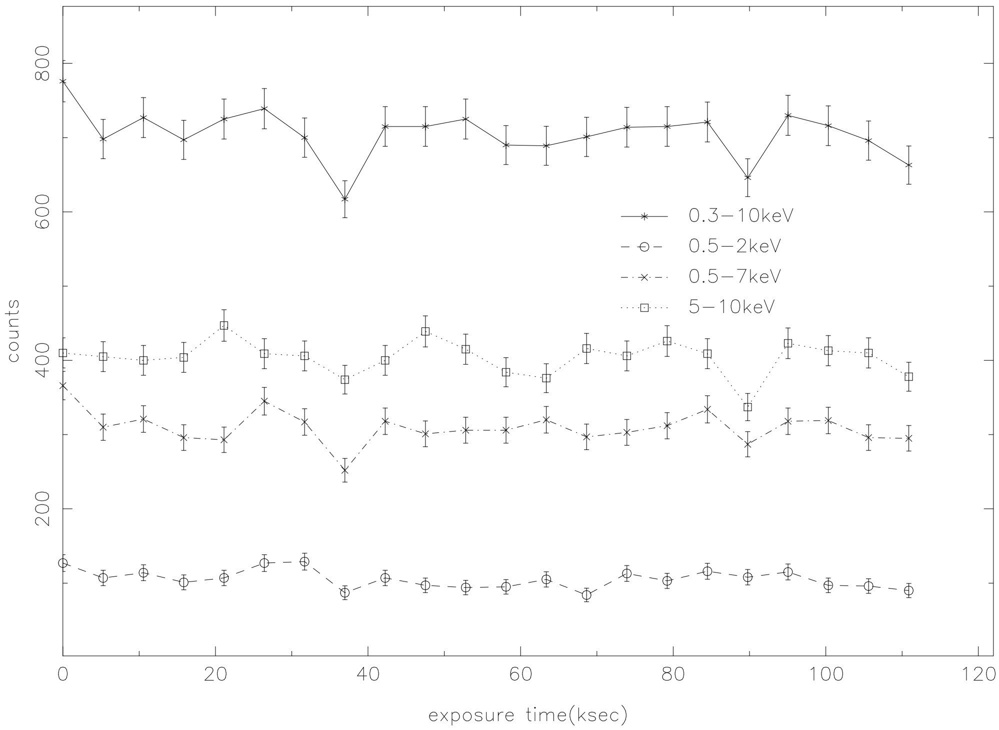

Figure 5: Counts per histogram file vs. elapsed time from beginning of exposure for the 0.3-10 keV, 5-10 keV, 0.5-2 keV, and 0.5-7 keV energy bands on S3 during obsid 964 (bottom). Each histogram file has an exposure time of 5.3 ksec.

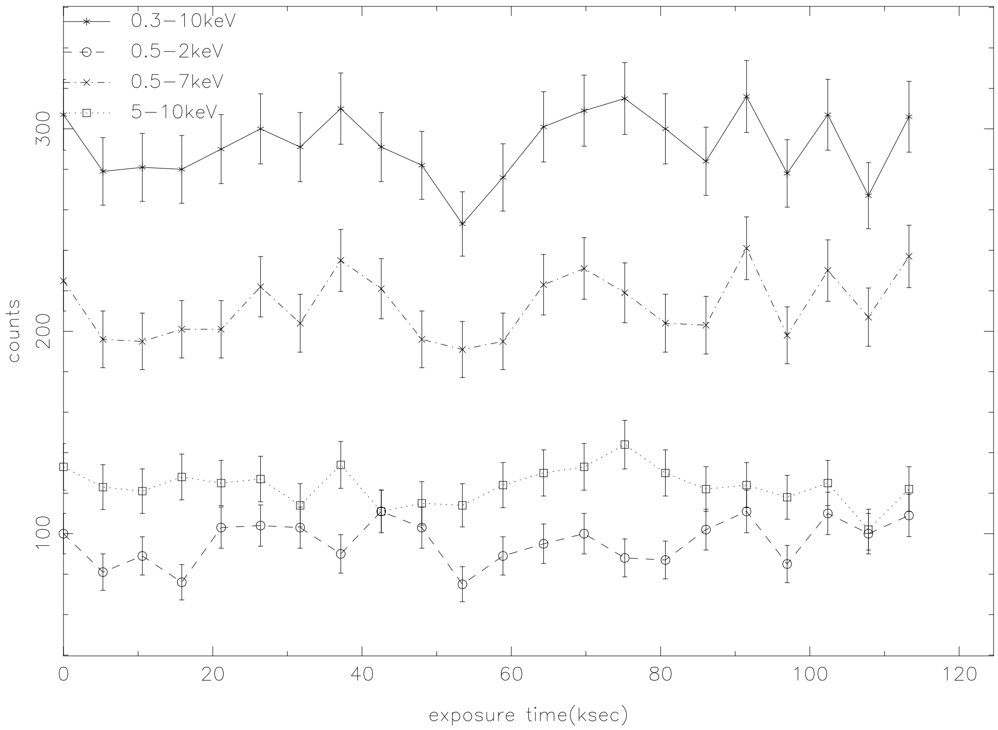

Figure 6: Counts per histogram file vs. elapsed time from beginning of exposure for the 0.3-10 keV, 5-10 keV, 0.5-2 keV, and 0.5-7 keV energy bands on I3 during obsid 964 (bottom). Each histogram file has an exposure time of 5.3 ksec.

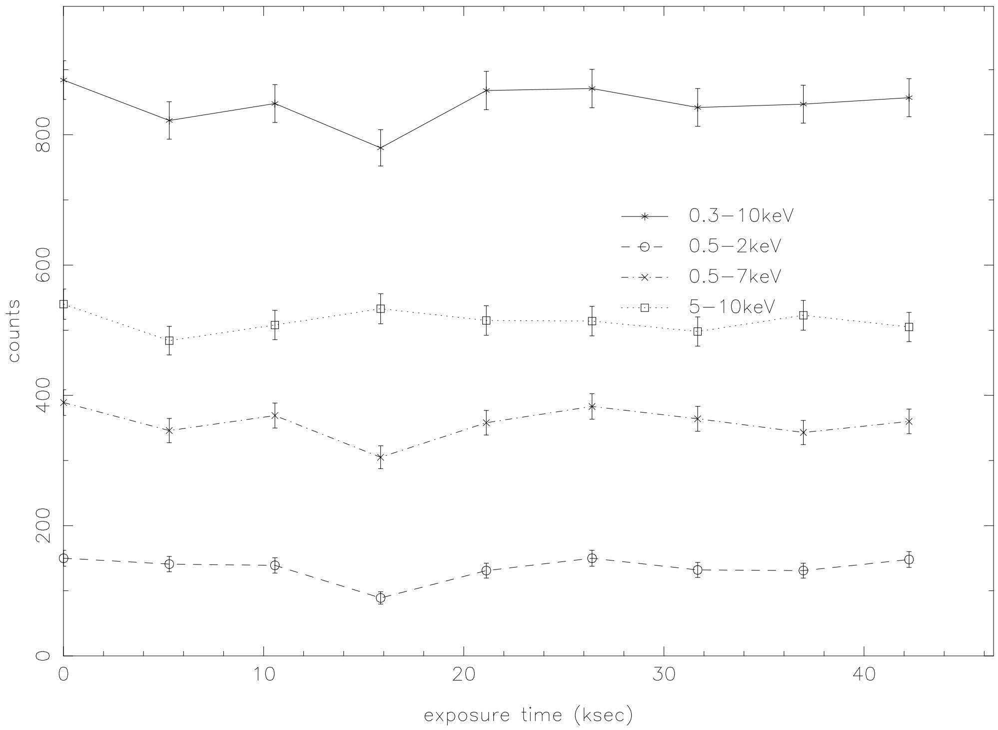

Figure 7: Counts per histogram file vs. elapsed time from beginning of exposure for the 0.3-10 keV, 5-10 keV, 0.5-2 keV, and 0.5-7 keV energy bands on S3 during obsid 27 (top). Each histogram file has an exposure time of 5.3 ksec.

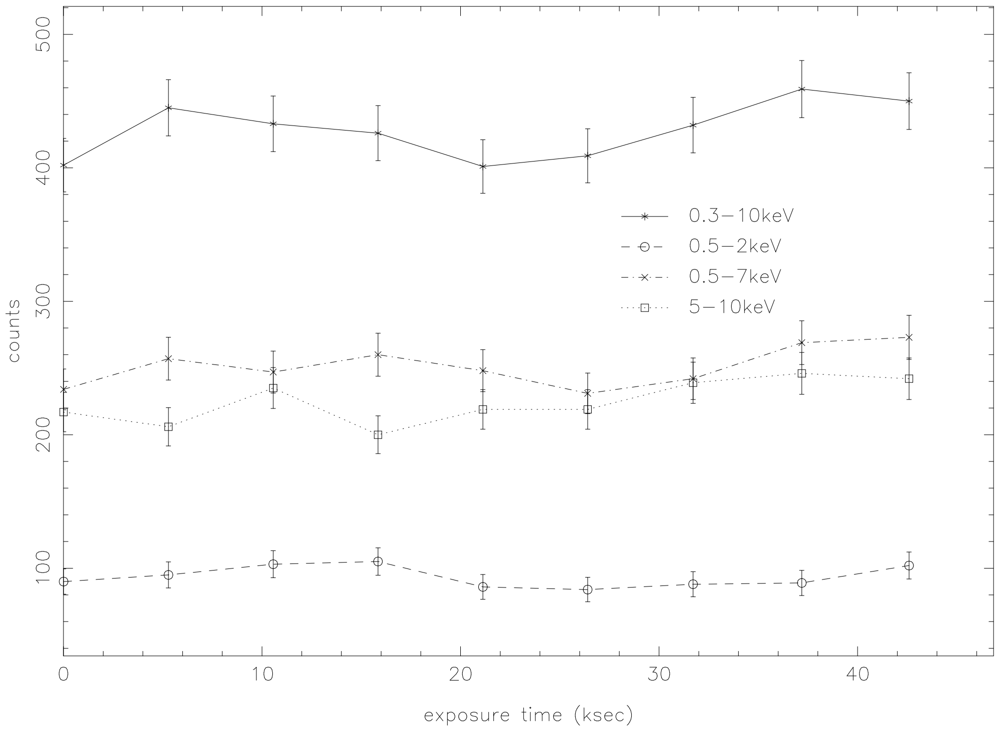

Figure 8: Counts per histogram file vs. elapsed time from beginning of exposure for the 0.3-10 keV, 5-10 keV, 0.5-2 keV, and 0.5-7 keV energy bands on I3 during obsid 27 (top). Each histogram file has an exposure time of 5.3 ksec.

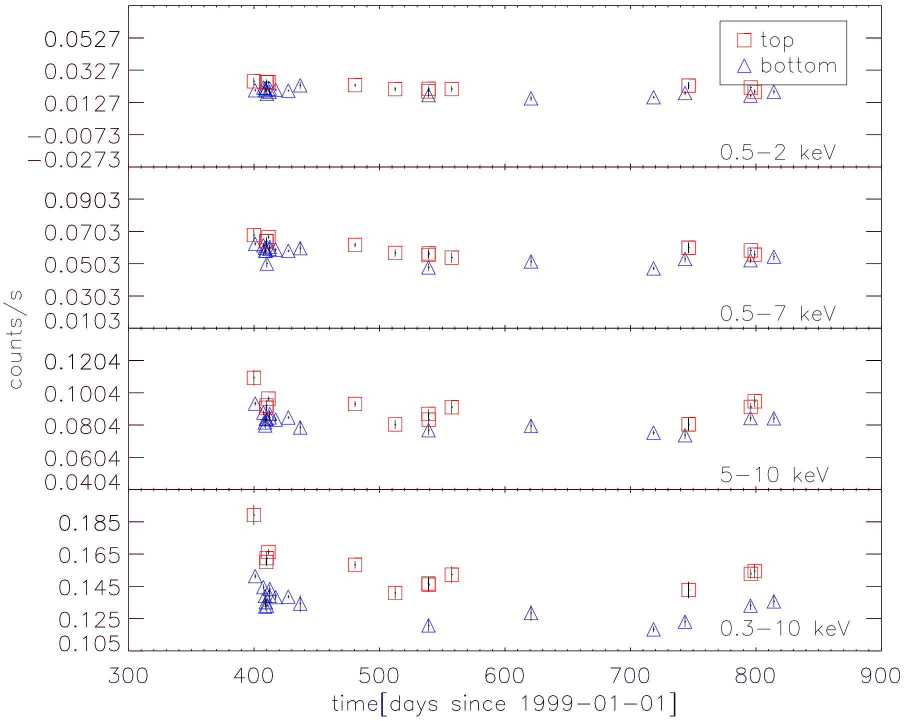

Figure 9: Days since 1999-01-01 vs. counts/s for a number of energy ranges on the S3 chip.

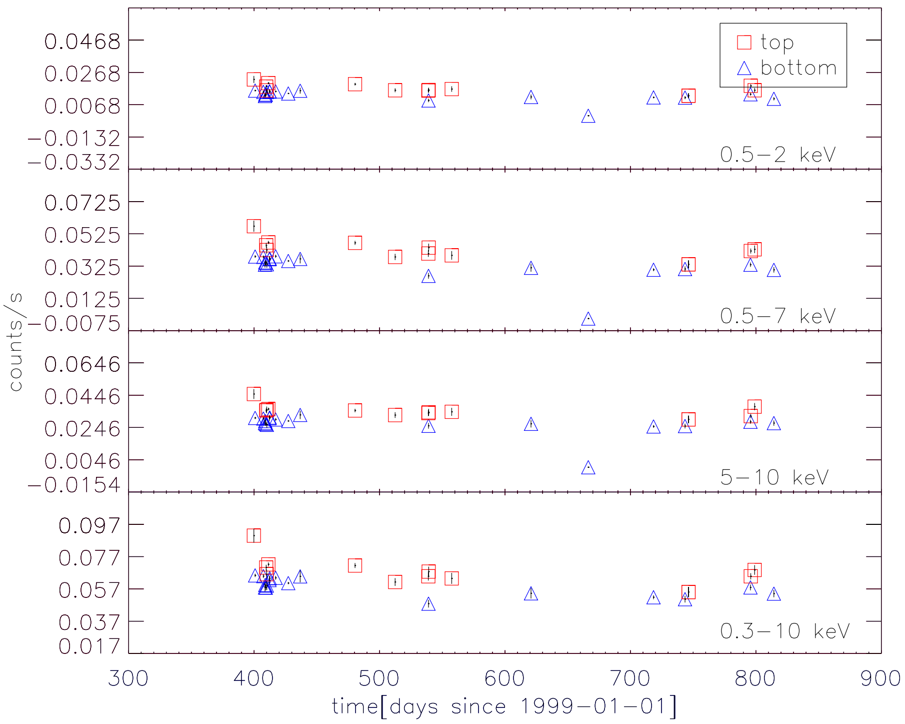

Figure 10: Days since 1999-01-01 vs. counts/s for a number of energy ranges on the I3 chip.

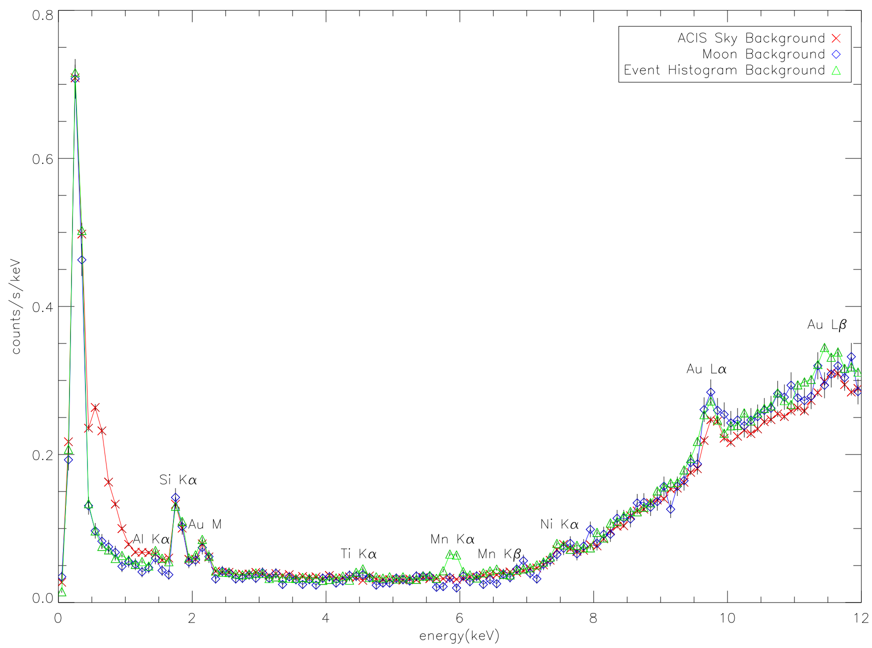

Figure 11: Overlay of ACIS sky background, moon background, and event histogram background for S3. Countrates in the histogram file background spectra have been corrected for the whole chip. All spectra are binned in units of 0.1 keV. Notable spectral features are labeled.

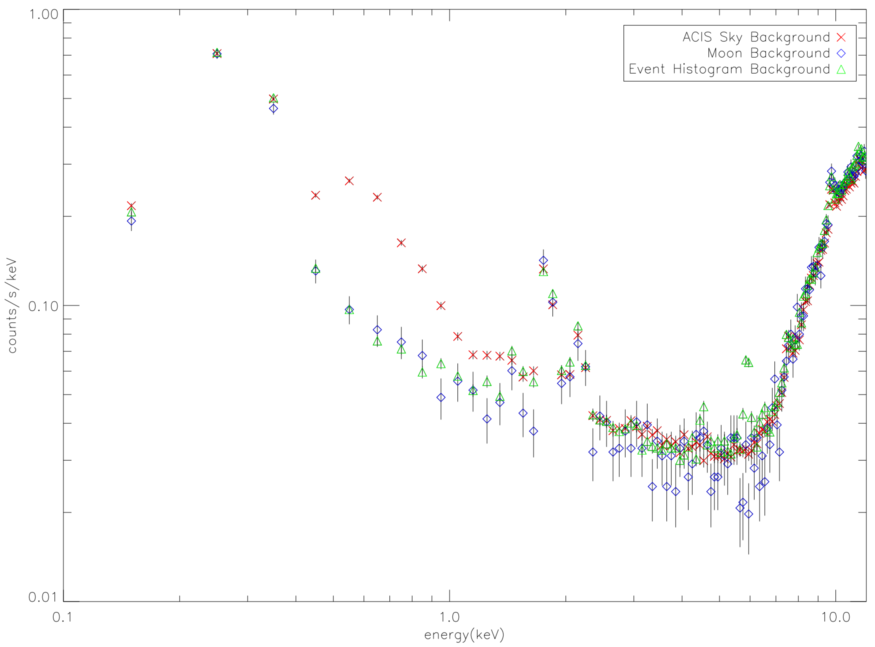

Figure 12: Overlay of ACIS sky background, moon background, and event histogram background for S3. Countrates in the histogram file background spectra have been corrected for the whole chip. All spectra are binned in units of 0.1 keV and axes are logarithmic.

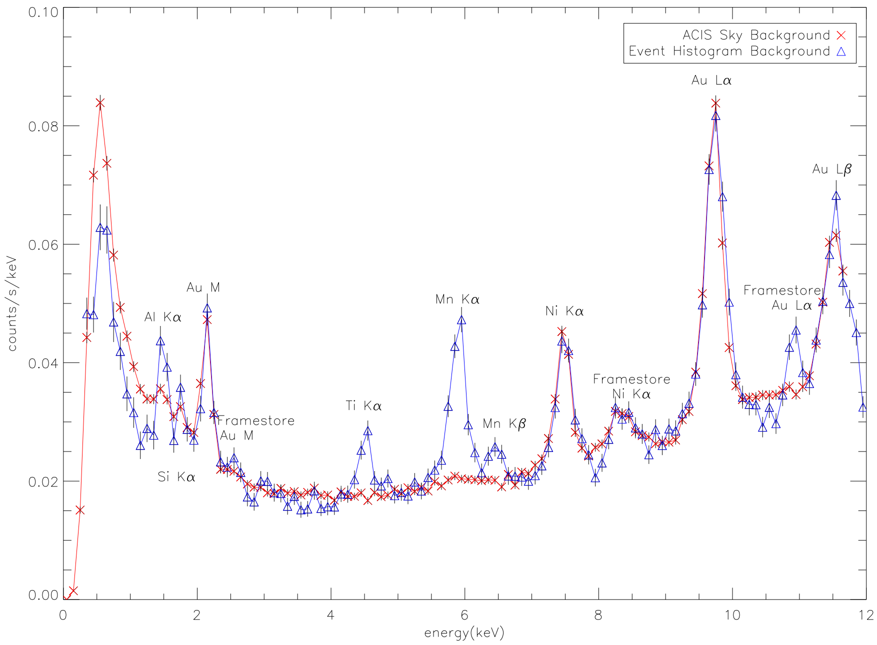

Figure 13: Overlay of ACIS sky background and event histogram background for I3. Countrates in the histogram file background spectra have been corrected for the whole chip. All spectra are binned in units of 0.1 keV. Notable spectral features are labeled.

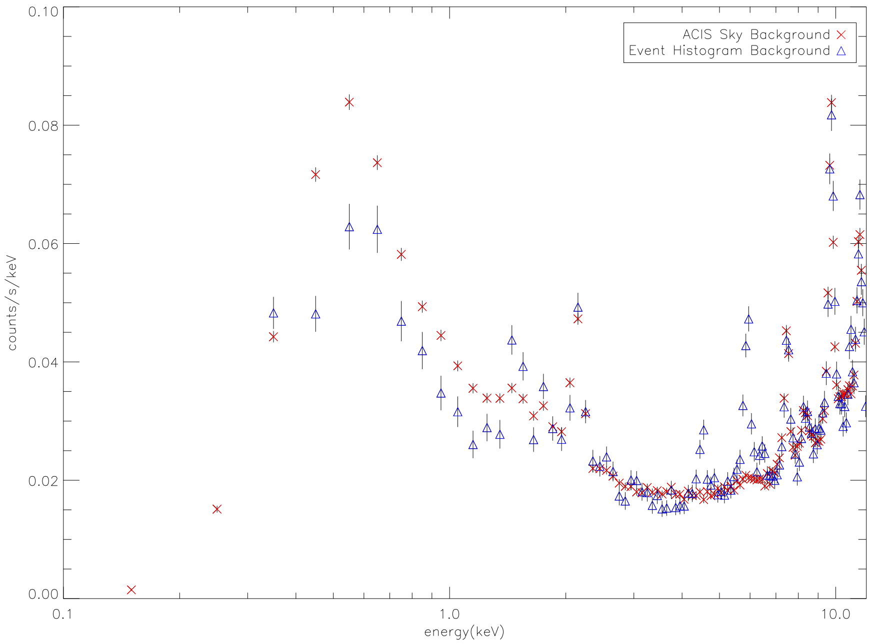

Figure 14: Overlay of ACIS sky background and event histogram background for I3. Countrates in the histogram file background spectra have been corrected for the whole chip. All spectra are binned in units of 0.1 keV and axes are logarithmic.

It is remarkable how good the agreement is between the Dark Moon spectra and the Event Histogram spectra. These data demonstrate that it is possible to observe with ACIS at the focus of the HRMA and to experience a negligible or no increase in the observed count rate due to low-energy protons. Before this measurement, it was not clear if there was always some low level of contamination present from low energy protons.

We overplot event histogram spectra with ACIS sky background spectra for I3 as well. Spectra on I3 (Figures 13 and 14) show similar trends. As on S3, we find an excess of emission in the ACIS sky background relative to the event histogram background at lower energies ($E \leq 1.5$ keV), as well as a number of spectral lines which appear in the event histogram background but not the ACIS sky background. We find a prominent Al Kα, Si Kα, and Au Mα, β complex in both backgrounds. The Al Kα line is stronger in the event histogram spectra than in the ACIS sky spectra. This is most likely a result of contamination from the external calibration sources. The Ti Kα, β and Mn Kα, β lines observed at $\sim$4.5 keV and $\sim$5.9 keV in the event histogram spectra are most likely also results of external calibration source contamination. At 9.7 keV and 11.5 keV, we find strong Au Lα,β lines in both spectra. Additional Ni and Au features appear at 2.5 keV, 8.5 keV, and 10.8 keV in the event histogram spectra but not in the ACIS sky background. These are from X-rays converted in the framestore region (which has no CTI) then gain corrected. (See Section II.)

5 REFERENCES

Baganoff, F. ACIS Memo 162, 1 September 1999.

Markevitch, M. 1999.
http://asc.harvard.edu/cal/Links/Acis/acis/Cal_prods/bkgrnd/current/index.html

Markevitch, M. 2001. http://icxc.harvard.edu/cal/earth/earth.html

Science Instrument Calibration Report for the AXAF CCD Imaging Spectrometer(ACIS)
http://cxc.harvard.edu/cal/Links/Acis/acis/WWWacis_cal.html